

Field emission from quasi-aligned SiCN nanorods

F. G. Tarntair, C. Y. Wen, L. C. Chen, J.-J. Wu, K. H. Chen, P. F. Kuo, S. W. Chang, Y. F. Chen, W. K. Hong, and H. C. Cheng

Citation: [Applied Physics Letters](#) **76**, 2630 (2000); doi: 10.1063/1.126431

View online: <http://dx.doi.org/10.1063/1.126431>

View Table of Contents: <http://scitation.aip.org/content/aip/journal/apl/76/18?ver=pdfcov>

Published by the [AIP Publishing](#)

Articles you may be interested in

[Enhanced electron field emission from plasma-nitrogenated carbon nanotips](#)

J. Appl. Phys. **111**, 044317 (2012); 10.1063/1.3688252

[Electron field emission from the Si nanostructures formed by laser irradiation](#)

J. Vac. Sci. Technol. B **28**, C2B11 (2010); 10.1116/1.3333435

[Diminish the screen effect in field emission via patterned and selective edge growth of ZnO nanorod arrays](#)

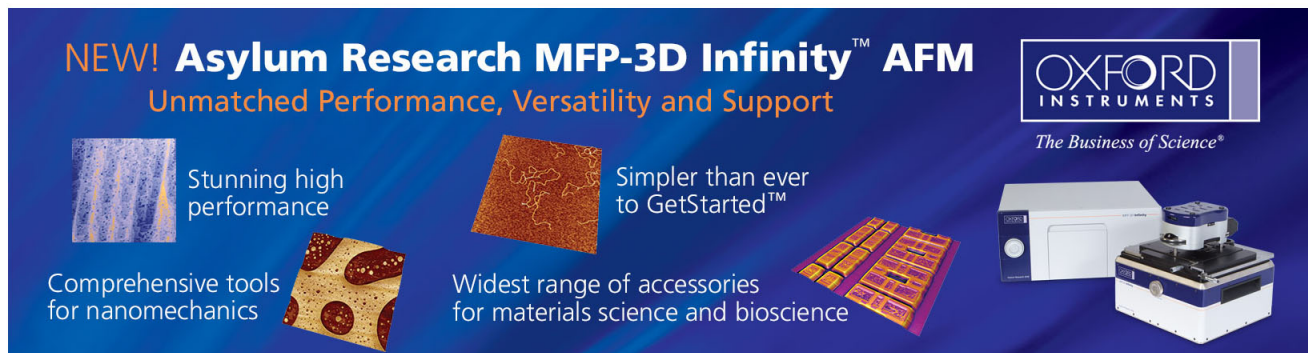
Appl. Phys. Lett. **95**, 153505 (2009); 10.1063/1.3247887

[Field emission from quasi-aligned aluminum nitride nanotips](#)

Appl. Phys. Lett. **87**, 073109 (2005); 10.1063/1.2009838

[Electron field emission from GaN nanorod films grown on Si substrates with native silicon oxides](#)

Appl. Phys. Lett. **86**, 082109 (2005); 10.1063/1.1869549

The advertisement features a dark blue background with white and orange text. At the top left, it reads 'NEW! Asylum Research MFP-3D Infinity™ AFM' in large white letters, with 'Unmatched Performance, Versatility and Support' in orange below it. To the right is the Oxford Instruments logo, which includes the text 'OXFORD INSTRUMENTS' and 'The Business of Science®'. Below the main text are four images: a textured surface, a circular pattern, a grid of small squares, and the AFM instrument itself. Each image is accompanied by a short text description: 'Stunning high performance', 'Simpler than ever to GetStarted™', 'Comprehensive tools for nanomechanics', and 'Widest range of accessories for materials science and bioscience'.

Field emission from quasi-aligned SiCN nanorods

F. G. Tarntair

Department of Electronic Engineering, National Chiao Tung University, Hsinchu, Taiwan

C. Y. Wen and L. C. Chen^{a)}

Center for Condensed Matter Sciences, National Taiwan University, Taipei, Taiwan

J.-J. Wu and K. H. Chen

Institute of Atomic and Molecular Sciences, Academia Sinica, Taipei, Taiwan

P. F. Kuo, S. W. Chang, and Y. F. Chen

Department of Physics, National Taiwan University, Taipei, Taiwan

W. K. Hong and H. C. Cheng

Department of Electronics Engineering, National Chiao Tung University, Hsinchu, Taiwan

(Received 29 November 1999; accepted for publication 25 February 2000)

We report on the preparation and field emission properties of quasi-aligned silicon carbon nitride (SiCN) nanorods. The SiCN nanorods are formed by using a two-stage growth method wherein the first stage involves formation of a buffer layer containing high density of nanocrystals by electron cyclotron resonance plasma enhanced chemical vapor deposition and the second stage involves using microwave plasma enhanced chemical vapor deposition for high growth rate along a preferred orientation. It should be noted that growth of the SiCN nanorods is self-mediated without the addition of any metal catalyst. Scanning electron microscopy shows that the SiCN nanorods are six-side-rod-shaped single crystals of about 1–1.5 μm in length and about 20–50 nm in diameter. Energy dispersive x-ray spectrometry shows that the nanorod contains about 26 at. % of Si, 50 at. % of C, and 24 at. % of N. Characteristic current–voltage measurements indicate a low turn-on field of 10 V/ μm . Field emission current density in excess of 4.5 mA/cm² has been observed at 36.7 V/ μm . Moreover, SiCN nanorods exhibited rather stable emission current under constant applied voltage. © 2000 American Institute of Physics. [S0003-6951(00)01117-7]

The recently discovered carbon nanotubes (CNT) have shown promising performance as electron field emitters since they exhibited high emission currents and very low turn-on voltages.¹ The extremely large field enhancement factor results from the sharp curvature of CNT is one of the key factors for the low threshold fields. However, poor emission stability of CNT has undermined their application in vacuum microelectronics.² A very sharp decay (a factor $\gg 10$) of the emission current for single-wall nanotubes has been reported.³ This degradation can be largely accounted for by progressive destruction of CNT during emission process.

In view of this, nanorods have the potential as field emitters due to the similarity in their geometric features with those of CNT but more stable structural properties. We report here a process on the preparation and field emission properties of SiCN nanorods. This class of material has two notable advantages. First, they can be deposited directly onto a substrate by using chemical vapor deposition (CVD) and second, their structures are naturally sharp and of nanosize, therefore, complicated treatments to sharpen geometric features commonly practiced on metal or Si surfaces can be avoided. The SiCN nanorods have a crystalline thin film counterpart, which has been reported recently as a superhard and wide band gap semiconductor,^{4–6} therefore, a great potential for blue and ultraviolet photoelectronic devices.

The SiCN nanorods were synthesized using a two-stage process. First, a SiCN buffer layer was deposited on Si (100) or (111) substrates using electron cyclotron resonance plasma enhanced CVD (ECR–CVD) of which the setup detail has been described previously.⁷ Then, the substrates were transferred to microwave plasma CVD (MW–CVD) reactor for the growth of nanorods. Detail process conditions are listed in Table I. Prior to MW–CVD process, a 10 min cleaning/etching of the substrate was performed using H₂ plasma. Scanning electron microscopy (SEM) and x-ray photoelectron spectroscopy (XPS) were used to characterize the resultant morphology, composition, and bonding state.

Typical cross-section-view SEM image of SiCN nanorods is shown in Fig. 1. This micrograph reveals a high density of quasi-aligned nanorods uniformly distributed over the entire substrate. The number density of the nanorods is around 10¹⁰ cm⁻². The nanorods exhibited a diameter in the range of 20–50 nm with typical length of 1–1.5 μm after

TABLE I. Typical process conditions for the growth of SiCN nanorods.

	1st stage	2nd stage
Deposition method	ECR–CVD	MW–CVD
(N ₂):(H ₂):(CH ₄):(SiH ₄) (sccm)	2.5:2.5:1.0:0.2	80:80:20:4
Microwave power (W)	1250	2000
Total pressure (Pa)	0.4	6250
Substrate temperature (°C)	650	1100
Reaction time (h)	6	3

^{a)}Author to whom correspondence should be addressed; electronic mail: chenlc@ccms.ntu.edu.tw

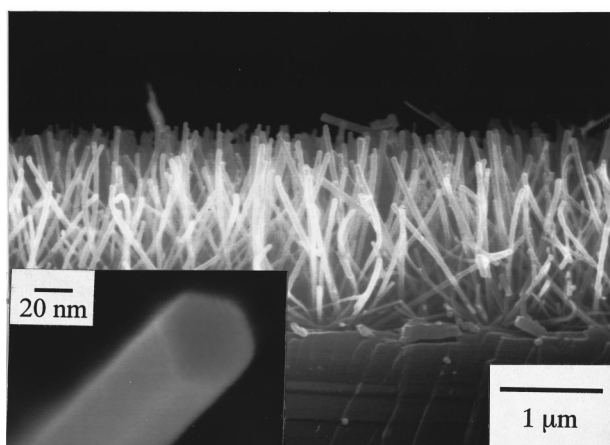


FIG. 1. Typical cross-section-view SEM image of the SiCN nanorods. The inset is a high-resolution SEM image that shows well faceted surfaces of each individual nanorod. The nanorod appears straight and has a six-sided cross section.

3 h deposition. It was found that while the length of the nanorod increased with growth time the diameter of the nanorod remained quite constant during the growth process. As can be seen from Fig. 1(b), there is a tendency for the long axis of the nanorods to grow in perpendicular to Si substrate although the angular distribution for the tilting of the rod axis away from the substrate normal is still quite large ($\sim 15^\circ$). High-resolution SEM image reveals well faceted surfaces of each individual nanorod. The nanorods appear straight and have a six-sided cross section. There is no visible reduction in cross section of SiCN nanorods, unlike the case for InAs and GaAs nanowires.^{8,9}

The energy dispersive spectrometry taken from the nanorod shows predominantly silicon, carbon, and nitrogen. Trace amount of oxygen was also observed, presumably due to surface contamination. It is also noted that the buffer layer contains the same chemical elements as the nanorod. Thus, the growth of SiCN nanorod is “self-mediated.” Unlike the case for the ordinary vapor-liquid-solid (VLS) process or catalyst-mediated growth, there is no evidence of metal inside or at the tip of the rod. The SiCN buffer layer deposited by ECR-CVD plays a key role on the growth of nanorod. An optimized buffer layer is a bilayer film wherein a nanocrystalline SiCN layer with a grain size around 20 nm is formed on top of the amorphous layer. A possible mechanism of this bilayer structure is that the nanocrystals are formed by the strain induced after a certain critical thickness of the amorphous film.¹⁰ The nanocrystals formed on top of the amorphous layer serve as the “seed” for the ensuing growth of nanorods. The process conditions in the second stage appear to favor growth along a preferred orientation, leading to very high aspect ratio of the rods. It should be emphasized that the two-stage process is essential for the growth of nanorod. The major difference between these two stages is that ECR-CVD may provide more abundant nucleation species due to its higher ionization fraction than MW-CVD.¹¹ Deposition of SiCN by MW-CVD without using ECR-CVD grown buffer layers led to polycrystalline film with low nucleation density and typical grain size of microns. On the other hand, deposition of SiCN by ECR-CVD alone led to continuous nanocrystalline film due to its

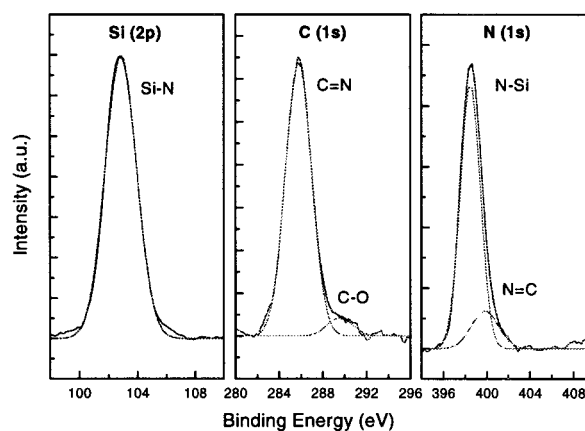


FIG. 2. High-resolution C(1s), N(1s), and Si(2p) XPS spectra of the SiCN nanorods.

high nucleation density. However, further study of the growth mechanism of the SiCN nanorods is needed.

Figure 2 depicts the high-resolution XPS scan of the C(1s), N(1s), and Si(2p) peaks. For calibration, Au(4f) peaks at 84 and 87.67 eV were used.¹² Tentative assignment of the carbon binding energies¹³ revealed predominantly “ sp^2 C–N” like bonding structure at 285.8 eV. A minor peak at 289.6 eV, attributable to C(1s)–O bonding structure, was also observed. For N(1s) peak, the 398.5 and 399.8 eV binding energies are related to the N(1s)–Si and the N(1s)– sp^2 C, respectively. The peak centered at 102.9 eV was assigned to Si(2p)–N bonding. Since the nanorods do not cover the surface completely, we cannot exclude the contribution from the buffer layer. However, it should be pointed out that there is no detectable C(1s)–Si signal at 282.8 eV, which is also confirmed by the absence of Si(2p)–C signal around 100.3 eV, indicating negligible Si–C bonds in the nanorods. This observation is consistent with our earlier report of the polycrystalline SiCN.¹⁴

Field emissions are characterized using parallel-plate configuration (with a spacing at about 30 μm) under a base pressure of 8.0×10^{-8} Torr and over a voltage sweep from 0 to 1100 V. Typical emission characteristics of a SiCN-nanorod sample is depicted in Fig. 3. An emission current of 4.5 mA/cm^2 at the maximum accessible voltage (i.e., applied field of 36.7 V/ μm) is observed. Furthermore, this material

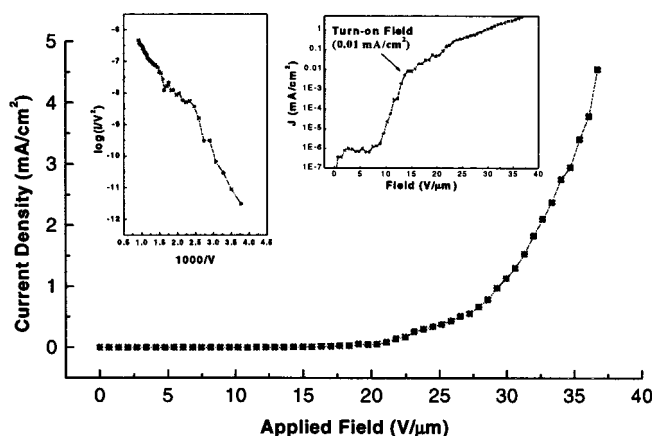


FIG. 3. Field emission J – E curve and the corresponding F–N plot of the SiCN nanorods.

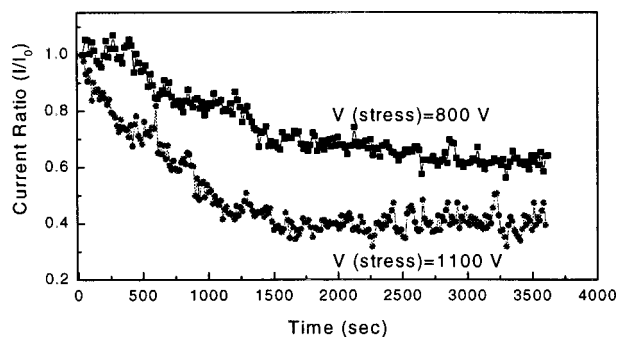


FIG. 4. Field emission stability (I/I_0 vs time) of a SiCN-nanorod sample tested with stress voltages at 800 and 1100 V.

also shows a low turn-on field at $10 \text{ V}/\mu\text{m}$, which is defined as the point where the current-voltage curve shows a sharp increase in the current density, or at $0.01 \text{ mA}/\text{cm}^2$ for convenience. The Fowler-Nordheim (F-N) description of the field emission originally established for metals is expressed as¹⁵

$$J = A \frac{F^2}{\phi} \exp\left(\frac{-B\phi^{3/2}}{F}\right), \quad (1)$$

where $A = 0.014$ and $B = 6.8 \times 10^9$ are constants. The rest in the F-N equation are: J the current density, ϕ the effective barrier height, $F = \beta V/d$ with V the voltage, d the cathode-to-anode spacing, and β the field enhancement factor that depends on the emitter geometry. For materials with field emission property that follows F-N theory, a plot of $\log(J/V^2)$ versus $1/V$ gives a straight line. The F-N plot is shown in the inset of Fig. 3.

It is difficult to determine the emission area, especially for materials of irregular surface morphology like nanotubes and nanorods. We assume an emission area equivalent to the anode area since we use parallel-plate configuration. The field enhancement factor, β , can be approximated by the length-to-radius ratio (l/r) of the rod. The SiCN samples exhibit l/r values in the range of 33–400 with an average value at about 60. The effective barrier heights estimated from the F-N plots are in the range of 0.12–0.02 eV with an average value at about 0.034 eV. These ϕ values are quite small as compared to diamond (0.37 eV).¹⁶ It is thus conjectured that small effective barrier heights of SiCN nanorods and/or large field enhancement factors are the key factors that account for their good electron emissions. Obviously, the field enhancement factor can be improved further by increasing the l/r value of the nanorods. Field enhancement factor higher than 1000 has been reported for CNT.³

The maximum accessible current density for SiCN nanorods varied from sample to sample, presumably, due to the difference in the number density as well as the geometry and orientation of the nanorods. Emission current density in excess of $1 \text{ mA}/\text{cm}^2$ can be routinely achieved. In order to increase the total current density a higher number density of nanorods is desirable. However, reduction in the enhancement of local electric field occurs as rod-to-rod distance approaches zero. An optimized structure for best emission property is one with an adequate spacing between the tips and yet having maximum numbers of tips per unit area.

While achieving highest emission current at lowest applied field is the goal in most field emission study, the long-

term stability of the emission is also essential. As shown in Fig. 4, at an applied voltage of 800 V ($\sim 26.7 \text{ V}/\mu\text{m}$), the I/I_0 values can be maintained at 65% after 3600 s of operation. Increasing the applied voltage to 1100 V accelerated the decay of the emission. Nevertheless, 40% of the initial current can still be maintained for SiCN nanorods after 3600 s of operation under such a high voltage. The emission stability of SiCN nanorods is much better in comparison to that of carbon-coated-Si microtips or CNT.^{17,18} For the latter two cases, the results of corresponding emission stability tests show a sharp decay to 25% and 15%, respectively, during the initial hundreds of seconds of operation. Furthermore, no structure damage of SiCN nanorods is observed from SEM investigation even after high voltage stress. Therefore, we suggest that the structure stability of SiCN nanorod is the key factor for good emission stability.

In conclusion, SiCN nanorods have been grown by a self-mediated two-stage growth technique, which is different from ordinary VLS method or catalyst-mediated growth of nanotubes/nanowires. Typical SiCN nanorods are of $1.2 \mu\text{m}$ in length and about 40 nm in diameter. The composition ratio of Si:C:N is about 1:2:1. Field emission characteristic of SiCN nanorods shows a low turn-on field with relatively high current density. The stability of field emission from such nanorods, in particular, is superior to that of other emitters such as CNT or carbon-coated-Si microtips. Due to the nanosize structure and robust nature, the SiCN nanorods show great potential for field emission device application.

¹Z. F. Ren, Z. P. Huang, J. W. Xu, J. H. Wang, P. Bush, M. P. Siegal, and P. N. Provencio, *Science* **282**, 1105 (1998).

²O. M. Küttel, O. Groening, C. Emmenegger, and L. Schlapbach, *Appl. Phys. Lett.* **73**, 2113 (1998).

³J. M. Bonard, J. P. Salvetat, T. Stockli, W. A. de Heer, L. Forro, and A. Chatelain, *Appl. Phys. Lett.* **73**, 918 (1998).

⁴L. C. Chen, C. K. Chen, S. L. Wei, D. M. Bhusari, K. H. Chen, Y. F. Chen, Y. C. Jong, and Y. S. Huang, *Appl. Phys. Lett.* **72**, 2463 (1998).

⁵L. C. Chen, K. H. Chen, S. L. Wei, J. J. Wu, T. R. Lu, and C. T. Kuo, *Thin Solid Films* **355–356**, 112 (1999).

⁶A. Badzian, T. Badzian, R. Roy, and W. Drawl, *Thin Solid Films* **354**, 148 (1999).

⁷K. H. Chen, J. J. Wu, L. C. Chen, C. W. Fan, P. F. Kuo, Y. F. Chen, and Y. S. Huang, *Thin Solid Films* **355–356**, 205 (1999).

⁸M. Yazawa, M. Koguchi, and K. Hiruma, *Appl. Phys. Lett.* **58**, 1080 (1991).

⁹K. Hiruma, T. Katsuyama, K. Ogawa, M. Koguchi, and H. Kakibayashi, *Appl. Phys. Lett.* **59**, 431 (1991).

¹⁰D. C. Nesting, J. Kouvetakis, and D. J. Smith, *Appl. Phys. Lett.* **74**, 958 (1999).

¹¹O. A. Popov, *Plasma Sources for Thin Film Deposition and Etching* (Academic, New York, 1994).

¹²R. J. Bird and P. Swift, *J. Electron Spectrosc. Relat. Phenom.* **21**, 227 (1980).

¹³D. Marton, K. J. Boyd, A. H. Al-Bayati, S. S. Todorov, and J. W. Rabalais, *Phys. Rev. Lett.* **73**, 118 (1994).

¹⁴L. C. Chen, D. M. Bhusari, C. Y. Yang, K. H. Chen, T. J. Chuang, M. C. Lin, C. K. Chen, and Y. S. Huang, *Thin Solid Films* **303**, 66 (1997).

¹⁵J. W. Gadzuk and E. W. Plummer, *Rev. Mod. Phys.* **45**, 487 (1973).

¹⁶S. P. Bozeman, P. K. Baumann, B. L. Ward, M. J. Powers, J. J. Cuomo, R. J. Nemanich, and D. L. Dreifus, *Diamond Relat. Mater.* **5**, 802 (1996).

¹⁷P. D. Kichambare, F. G. Tartair, L. C. Chen, K. H. Chen, H. C. Cheng, *J. Vac. Sci. Technol. B* (to be published).

¹⁸K. H. Chen, J. J. Wu, L. C. Chen, C. Y. Wen, P. D. Kichambare, F. G. Tartair, P. F. Kuo, S. W. Chang, and Y. F. Chen, *Diamond Relat. Mater.* (to be published).